SHC 2013, International Conference on Solar Heating and Cooling for Buildings and Industry September 23-25, 2013, Freiburg, Germany

Thermal analysis of flat and transpired solar facades

Hoy-Yen Chan[a]*, Jie Zhu[b], Mohd Hafidz Ruslan[a], Kamaruzzaman Sopian[a], Saffa Riffat[b]

[a]Solar Energy Research Institute (SERI), National University of Malaysia, 43600 Bangi, Selangor Darul Ehsan, Malaysia.
[b]Department of Architecture and Buil Environment, Faculty of Engineering, University of Nottingham, University Park, Nottingham, NG7 2RD, United Kingdom

Abstract

Building integrated solar technologies is important not only to reduce energy consumption and carbon emissions but also to help to make the technologies more economically feasible and challenge the creativity of architects in designing buildings. In this paper, two types of solar facades for heating purposes were studied: flat and transpired aluminium plates. Mathematical models of the thermal performance of these plates were developed and verified through experiments. The thermal performances were then compared in terms of heat gains and losses under the same operational conditions. It is found that the transpired design is able to reduce heat losses and hence achieve better heat transfer: the efficiencies for the flat and transpired facades are about 30% and 80% respectively.

1. Introduction

Ventilated solar facade has become one of the attempts to reduce the space heating energy consumption. In order to make this technology common practice in the construction industry, it is important to design the solar facade properly. Basically thermal characteristic studies for different designs of solar facades have been carried out by three methods: experimental measurements [1-3], numerical simulations [4,5], and visualisation studies [6,7]. The solar facades in the present study aim to analyse the thermal characteristic of solar facades by comparing two different

————

* Corresponding author. Tel.: +60-389-118-581; fax: +60-389-118-574.
  E-mail address: hoyyen.chan@ukm.my

Nomenclature

A_p	Surface area of transpired plate, m^2
c_p	Heat capacity, $Jkg^{-1}K^{-1}$
D	Plenum depth, m
G	Suction mass flow rate per unit area, $kgs^{-1}m^{-2}$
h	Heat transfer coefficient, $Wm^{-2}K^{-1}$
I	Solar irradiance, Wm^{-2}
k_1	Thermal conductivity of sand-tile wall, $1.07\ Wm^{-1}K^{-1}$ [8]
k_2	Thermal conductivity of insulation layer, $0.023\ Wm^{-1}K^{-1}$ [8]
L_1	Thickness of sandtile wall, m
L_2	Thickness of insulation layer, m
$\dot{m}$	Mass flow rate, kgs^{-1}
q	Heat flux, Wm^{-2}
Q	Heat, W
T	Temperature, K
U_L	Overall heat transfer coefficient between sand-tile wall and insulation layer, $Wm^{-2}K^{-1}$

Greek symbols

α_p	Absorptivity
ε_{HX}	Heat exchange effectiveness, %
ε_p	Emissivity
$\eta;\ Eff$	Efficiency, %

Subscripts

a	Ambient air
$bp\text{-}air$	Between back-of-plate of transpired plate and plenum air
$conv$	Convection
$c,trans$	Convection between transpired plate and ambient air, normal flow heat transfer of transpired plate
f	Air in plenum; convection between back-of-plate and plenum air
$f,trans$	Convection between back-of-plate of transpired plate and plenum air, vertical flow heat transfer of transpired plate
i	Air entering into plenum, air temperature at the bottom of plenum, K (transpired plate)
in	Inlet
$loss,wall\text{-}room$	Heat loss from sand-tile wall to wall attached to the room
out	Outlet
p	Plate
$p\text{-}air$	Between transpired plate and ambient air
$p\text{-}sur$	Between plate and surrounding
r	Wall attached to room
rad	Radiation heat transfer from plate to surrounding
$trans$	Transpired plate
w	Sand-tile wall

designs (Fig. 1): a flat plate (without hole) and a transpired façade. The study was carried out experimentally to validate the mathematical models. The thermal performance analyses including heat losses are compared and discussed for both designs.
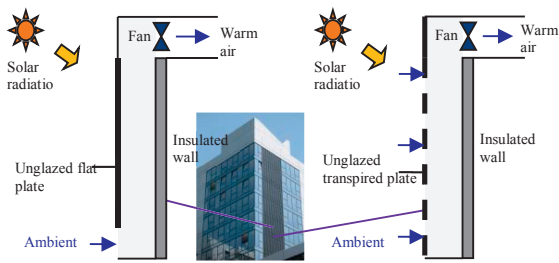
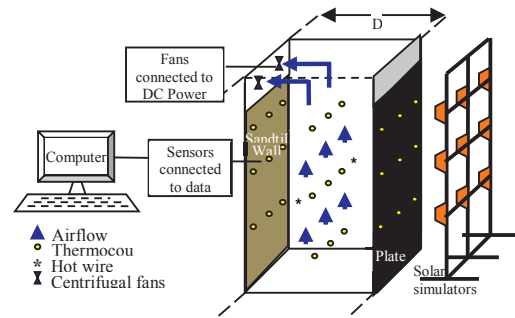Fig. 1. Side view of solar façade heating system

Fig. 2. Schematic diagram of experimental set up

2. Methodology

2.1 Experimental set up

Both the flat and transpired plate collectors shared the same experimental set-up (Fig. 2). Both plates were made from black painted aluminium sheet, 2m in height, 1m wide, and 0.001m in thickness. The porosity (ratio of hole area to total surface area) of the transpired plate was 0.84%, with a circular hole diameter of 0.0012m, a pitch distance of 0.012m in triangular geometry.

Two fans were installed at the air outlet. The heating system with flat plate collector drew air from the opening at the bottom of the plenum and delivered it into the room through an opening at the top of the plenum. The dimensions of the openings at the bottom and top of the plenum were 0.167m × 1.0m and 0.23m × 1.0m, respectively. In order to reach a steady state, temperatures were not recorded until two hours after the test began, by which time constant temperatures had been achieved. Temperatures were then taken every minute for the next 30 minutes. Air velocities were measured by hot wire anemometers at the centreline of the plenum and at the outlet of the plenum. Experiments were repeated for a heating system with transpired plate collector by replacing the porous plate with the flat plate. In this case, the opening at the bottom was closed so that the air was drawn through the holes and delivered into the room through the opening at the top of the plenum.

2.1.2 Heat transfer at the insulated sand-tile wall

The backside of the sand-tile wall was insulated with a rigid polyisocyanurate foam board with glass fibre. This section is to verify that the heat loss from the sand-tile wall to the surface of the room is negligible. Fig. 3 is the diagram of heat transfer of the wall from T_w to T_r. The heat flux equation is:

$$q_{loss,wall-room} = U_L(T_w - T_r) , \tag{1}$$

where $U_L = 1/(L_1/k_1 + L_2/k_2)$

Temperatures of T_w and T_r were measured by experiment, and the heat losses were calculated. Results show that for all the experiments that were carried out, the heat losses were less than 0.5% of the total useful energy delivered for plenum depths of 0.20m, 0.25m and 0.30m (Fig. 4). Thus, heat transfer at the insulated sand-tile wall is negligible. Therefore, hereafter, all the energy balance equations that involved the insulated sand-tile wall will be ignored in the future sections.
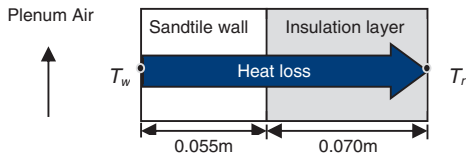
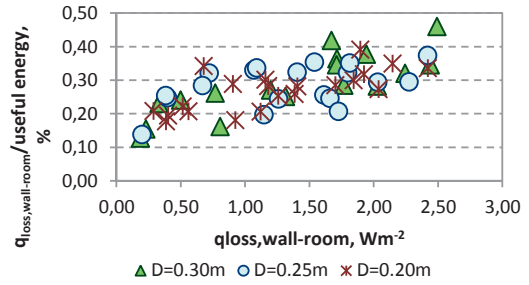Fig. 3. Heat transfer illustration of insulated sandtile wall.

Fig. 4. Heat loss to sandtile wall over total useful energy.

2.2 Mathematical model

2.2.1 Heat transfer of the flat plate solar facade

Some assumptions have been made while developing the mathematical model:
  i)   The airflow rate is assumed to be constant throughout the plenum.
  ii) All the measured temperatures that were used in the energy balance equations were assumed to be the constant temperatures after reaching a steady state.

2.2.1.1   Energy balance equations for the flat plate facade

The energy balance equations are established and illustrated in Fig. 5. Eq. 2 shows the overall energy balance of the system:

$$\dot{m}c_p(T_{out} - T_{in}) = I\alpha_p A_p - Q_c - Q_r \tag{2}$$

The left-hand side of this equation represents the useful energy collected. The first term on the right-hand side is the solar energy absorbed by the aluminium black plate. The second and third terms are the heat losses to the surrounding via radiation and convection respectively. Hence, the heat flux equations for the plate and plenum are as follows:

Flat plate:

$$I\alpha_p A_p = h_c(T_p - T_a) + h_f(T_p - T_f) + h_r(T_p - T_a), \tag{3}$$

where $T_a = T_{in}$.

Plenum air:

$$M(T_{out} - T_a) = h_f(T_p - T_f), \tag{4}$$

where $M = (\sum \dot{m} c_p)/A_p$; $A_p = HL$; $\dot{m} = \rho_f v_f DL$; and $v_f = V_{fan}/DL$; $T_f = (T_{out} + T_{in})/2$.
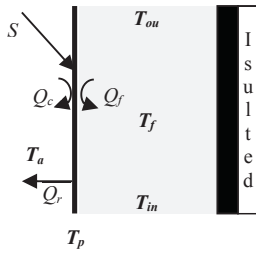
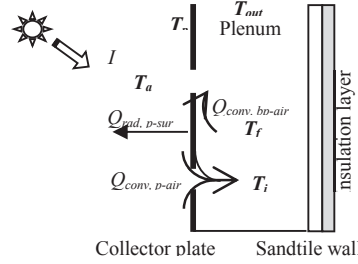Fig. 5. Heat transfers of flat plate solar collector.

Fig. 6. Heat transfers of transpired solar collector.

2.2.1.2 Mean temperature matrix for the flat plate facade

Equations 3 and 4 can be simplified to Eq. 5 and 6 respectively, and form a 2×2 matrix, equation 7, as follows:

$$(h_c + h_f + h_r)T_p - h_f T_f = S + h_c T_a + h_r T_a \tag{5}$$

$$h_f T_p - (h_f + 2M)T_f = -2MT_a \tag{6}$$

$$\begin{bmatrix} h_c + h_f + h_r & -h_f \\ h_f & -(h_f + 2M) \end{bmatrix} \begin{bmatrix} T_p \\ T_f \end{bmatrix} = \begin{bmatrix} S + h_c T_a + h_r T_a \\ -2MT_a \end{bmatrix} \tag{7}$$

Hence, rewriting Eq. 11 by using the matrix inversion method gives:

$$\begin{bmatrix} T_p \\ T_f \end{bmatrix} = \begin{bmatrix} h_c + h_f + h_r & -h_f \\ h_f & -(h_f + 2M) \end{bmatrix}^{-1} \begin{bmatrix} S + h_c T_a + h_r T_a \\ -2MT_a \end{bmatrix} \tag{8}$$

Eq. 8 is then solved by an iteration method, and the iteration process is continued until the convergence value is better than 10^{-6}.

2.2.2 Heat transfer of the transpired solar facade

   This concept is different from that used by most researchers [9-11], who believe that there is no vertical flow heat transfer. Although detail discussions on vertical flow are beyond this paper, more details can be found in [12]. Due to the complication of the heat transfer process, some assumptions have been made:
   i) The radiation heat loss over the surface of the transpired plate is everywhere constant, as it has been proved that it has only a modest effect on the flow distribution [13].
   ii) The experimental tests were carried out in a closed laboratory, and the convection losses to the ambient are negligible – this has been verified by a previous study [14].
   iii) There is no reverse flow across the plate, as the face velocities in this study are higher than $0.0125 ms^{-1}$[13].
   iv) The temperatures that are measured by the thermocouples, which have the same height as the first row of holes from the bottom, are taken as air the temperatures reached in the plenum after passing through the holes.
   v) The air properties remain the same throughout the plenum (the maximum air temperature difference between the inlet and outlet is about 10K in this study).

2.2.2.1 Energy balance equations for the transpired plate facade

   The energy balance equations are established for two components of the system: the unglazed transpired plate and the air in the plenum. The heat transfers of the system are as shown in Fig. 6. The fan-assisted system draws ambient air through the holes so that heat, which would otherwise be lost by convection, is captured by the airflow

into the plenum. Thus, there will be only very small amounts of convection heat loss to the ambient, which can indeed be neglected [10,11,15]. The energy balance and heat flux equations are in Eq. 9 and 10 respectively.

Unglazed transpired facade:

$$I\alpha_p A_p = Q_{conv,p-air} + Q_{conv,bp-air} + Q_{rad,p-sur} \qquad (9)$$

$$\left(h_{c,trans} + h_{f,trans} + h_r\right)T_p - \left(h_{c,trans} + h_{f,trans}/2\right)T_i - \left(h_{f,trans}/2\right)T_{out} = I\alpha_p + h_r T_a \qquad (10)$$

Plenum air:

The ambient air, which is heated by the front and hole of the transpired plate, is further heated through the back of the plate when flowing throughout the plenum. The energy balance and heat flux equation of the air in the plenum are as follows:

$$\sum \dot{m} c_p (T_{out} - T_i) = Q_{conv,bp-air} \qquad (11)$$

$$h_{f,trans} T_p + \left(G c_p - h_{f,trans}/2\right)T_i - \left(G c_p + h_{f,trans}/2\right)T_{out} = 0 \qquad (12)$$

where $G = \sum \dot{m}/A_p$; and $T_f = (T_i + T_{out})/2$.

The convection heat transfer equations can be written in term of mass flow rate and heat flux, as shown in Equations 13 and 14 respectively, and are simplified as Eq. 15.

$$q_{conv,p-air} = \sum \dot{m} c_p (T_i - T_a)/A_p \qquad (13)$$

$$q_{conv,p-air} = h_{c,trans}\left(T_p - T_i\right) \qquad (14)$$

$$h_{c,trans} T_p - \left(G c_p + h_{c,trans}\right)T_i = -G c_p T_a \qquad (15)$$

2.2.2.2 Mean temperature matrix for the transpired facade

Equations 10 to 15 can be written in a 3×3 matrix form:

$$\begin{bmatrix} \left(h_{c,trans} + h_{f,trans} + h_r\right) & -\left(h_{c,trans} + h_{f,trans}/2\right) & -\left(h_{f,trans}/2\right) \\ h_{f,trans} & \left(G c_p - h_{f,trans}/2\right) & -\left(G c_p + h_{f,trans}/2\right) \\ h_{c,trans} & -\left(G c_p + h_c\right) & 0 \end{bmatrix} \begin{bmatrix} T_p \\ T_i \\ T_{out} \end{bmatrix} = \begin{bmatrix} I\alpha_p + h_r T_a \\ 0 \\ -G c_p T_a \end{bmatrix} \qquad (16)$$

The matrix equation is then solved by an iteration method, and the iteration process is continued until the convergence value is better than 10^{-6}.

2.3. System performance evaluation

System efficiency

The efficiency of the heating system is the ratio of the useful energy delivered to the total solar energy input on the plate, and it is given as Eq. 17.

$$\eta = \sum \dot{m} c_p (T_{out} - T_a)/\left(I A_p\right) \qquad (17)$$

Heat exchange effectiveness

The heat exchange effectiveness of the solar collector is defined as the ratio of the actual temperature rise of air to the maximum possible temperature rise [14]:

$$\varepsilon_{HX} = (T_{out} - T_a)/\left(T_p - T_a\right) \qquad (18)$$

Percentage difference

If x_1 and x_2 are the values taken from the model and the experiment respectively, the percentage difference is calculated as:

$$Percentage\ difference = \left|\frac{x_1 - x_2}{(x_1 + x_2)/2}\right| \times 100\% \qquad (19)$$

3. Results comparison of the measured and modelled

3.1 Flat plate

The results comparison is analysed in terms of heat exchange effectiveness (Fig. 7). After taking account of the ±16% of the experimental error, all the modelled efficiencies are within the acceptance ranges, and hence the model is appropriate to be used for the simulation study in the next section.
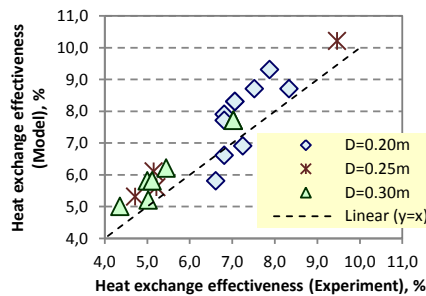

Fig. 7. Comparison of heat exchange effectiveness between experimental results and present modelling for the flat plate

3.2 Transpired plate

From Kutscher's study [14], the only heat transfer correlation for the transpired solar collector was developed from the heat exchange effectiveness (ε_{HX}), thus ε_{HX} is chosen for the comparison between the modelled and measured results. From Fig. 8a, the values of ε_{HX}, which are calculated from both experiment and the present model methods give close results with the highest percentage difference of 7.9% for three different plenum depths at various solar intensities and suction mass flow rate values. Nonetheless, Kutscher's study assumed that the temperature of the vertical flow was constant, which contrasts with the present study where the vertical flow temperature increases gradually throughout the plenum. Thus, in order to further confirm the accuracy of the present model, a simulation study using Kutscher's model was carried out to compare with the present model. In terms of total rise in air temperature ($T_{out} - T_a$), the present model shows comparable results to Kutscher's model (Fig. 8b) for solar radiation intensities above 400Wm^{-2}. Relatively, Kutscher's model gives higher percentage differences (>14%) than the present model (<8%) at 307Wm^{-2} of solar radiation intensity compared to the experimental results. Therefore, the present model is chosen and to be used for the simulation study in the next section.

4. Thermal performance comparisons

The thermal performances of both flat and transpired plates are evaluated by using the models that have been developed. The input parameters for both plates are the same: solar radiation intensity, ambient air temperature, airflow rate, plate area and plenum depth.
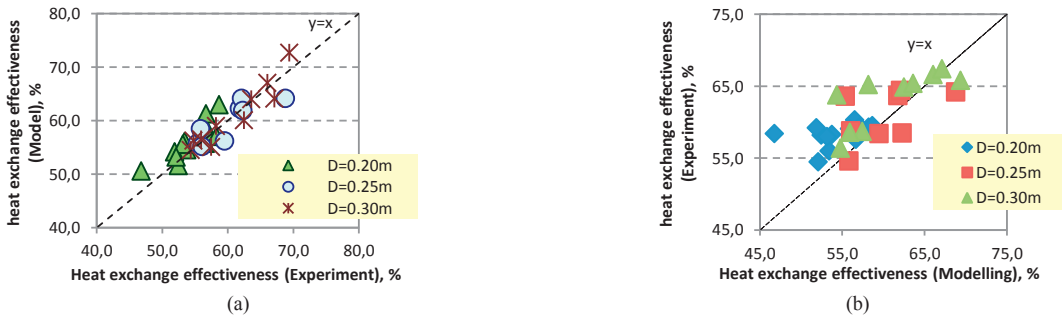
Fig. 8. Comparison of heat exchange effectiveness between experimental results and (a) present modelling; (b) Kutscher's model for the transpired plate

4.1 Heat losses

The transpired plate has better heat transfer compared to the flat plate. This can be seen by comparing the flat plate to the transpired plate, whereby higher rise in air temperature (Fig. 9a) for transpired type although the values of T_p are lower than the flat type (Fig. 9b). The useful heat flux that is delivered by the system with flat plate is only about 30% of the total solar heat flux that been absorbed by the plate, while for the transpired plate it is about 84%. Fig. 10(a) shows the rises in heat fluxes of the flat plate when the solar radiation intensity is increased from 300 to 800Wm^{-2} at a constant airflow rate of 300m^{3}hr^{-1}. The losses to the ambient are increased and in particular, q_r has the greatest increase. As for q_f, although it increases with solar radiation intensity, the amount of rise is smaller than the losses (the sum of q_r and q_c). This explains why the values of the flat plate temperature increase greatly but there is only a small rise in air temperature. On the other hand, for the transpired plate, the rises in q_c and q_f are greater than that for q_r (Fig. 10b). This results in a large increase in q_d (the sum of q_c and q_f). The heat losses to ambient of the flat plate are partly caused by convection heat loss, while for the transpired plate the ambient convection heat loss can be ignored, whereby most of the heat which indeed would be lost to the ambient has been sucked into the plenum through the small holes. This reduces the total heat losses and hence gives a better heat transfer for the transpired design.

4.2 System performance comparisons of solar air heaters

For solar collector applications, system efficiency is crucial in terms of heating performance. The efficiencies for both designs at various suction mass flow rates and solar intensities are as shown in Fig. 11.
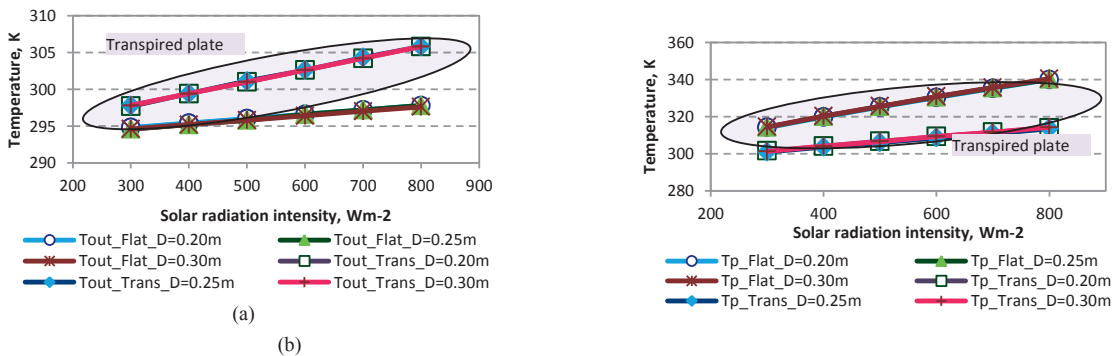

Fig. 9. Simulated values of (a) T_{out} and (b) T_p of flat and transpired plates for plenum depths of 0.20m, 0.25m and 0.30m.
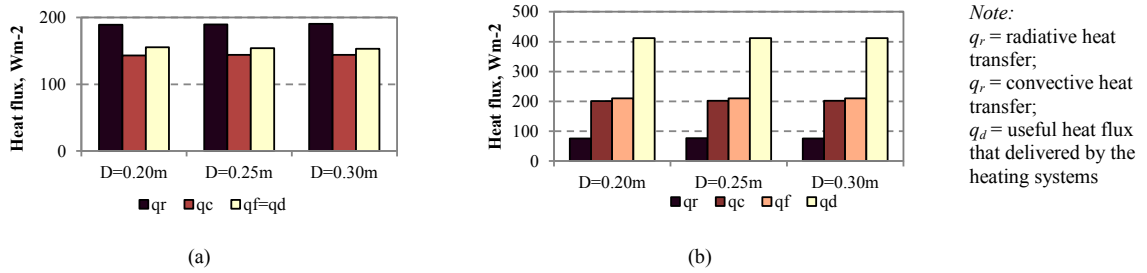
Note:

q_r = radiative heat transfer;

q_r = convective heat transfer;

q_d = useful heat flux that delivered by the heating systems

(a)   (b)

Fig. 10. Rise in heat fluxes of (a) flat and (b) transpired plates when the solar radiation intensity increases from 300 to 800Wm^{-2}.
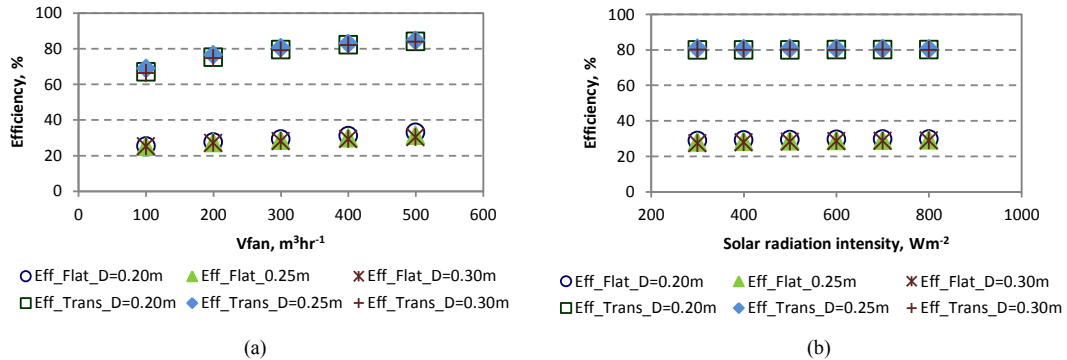

(a)   (b)

Fig. 11. System efficiencies at various (a) airflow rates and (b) solar radiation intensities

Results show that a higher suction mass flow rate gives higher system efficiency. For the transpired plate, the efficiency of the system is 67–83%, which is equivalent to temperature rises of 9–13K. For practical applications, operating parameters would very much depend on the application purposes of the heating system. Typical suction velocities range from 0.01ms^{-1} for desiccant regeneration to 0.05ms^{-1} for preheating ventilation air [15]. Since the system efficiency is high, for applications that require a lower rise in air temperature, the solar collector can be painted with a variety colour choices by choosing the appropriate absorptivity and emissivity values of the plate. In terms of aesthetics, this is one of the most important aspects for building integration technologies.

The system efficiency of the present system is compared to various designs of solar air heaters and they are as shown in Table 1. The present design gives the highest efficiency among all the reported maximum values of efficiency. As well as the benefit of low convection heat loss to the ambient of the present design, all the active solar air heaters are glass covered to form a channel between the glass and the absorber for the air passing through it, whereas the present design is the unglazed type, so it gives higher thermal performance. The present design not only manages to achieve higher system efficiency, but also benefits in terms of system simplicity and lower cost.

Table 1. System efficiency comparisons among some reported solar air heaters.

Solar air heater	System efficiency	References
Present (maximum)	0.82	
Transpired solar collector	0.78	[15]
Vertical flat plate	0.50	[16]
Flat plate	0.49	[17]
Single pass with double ducts	070	[18]
Double pass with aluminium cans	0.70	[19]
Wire-mesh packing	0.46-0.68	[20]

5. Conclusions

The thermal performances of two solar facades – flat and transpired black aluminium plates – were investigated through mathematical models, which have been verified by experimental results. The results show that the efficiency of transpired design is 50% higher than the flat plate under the same climate conditions. This is because the transpired plate is able to reduce the convection and radiation heat losses. The convection heat flow between the ambient and the plate is forced into the plenum through the holes, thus this heat that indeed would be lost to the ambient has been contributed as part of the useful heat of the system. In addition, under the same operational conditions, the flat plate gives higher surface temperature but lower output air temperature. This indicates that the transpired design has better heat transfer. Therefore, this reduces the surface temperature of the transpired plate and hence the radiation heat loss. Due to the high efficiency of the transpired solar facade that is close to 80%, it provides more flexibility to architects in terms of aesthetics, as a variety colour choices is possible, especially in moderate climate countries.

References

[1] Chen W, Liu W. Numerical analysis of heat transfer in a composite wall solar-collector system with a porous absorber. Appl Energ 2004;78(2):137-49.
[2] Burek SAM, Habeb A. Air flow and thermal efficiency characteristics in solar chimneys and Trombe Walls. Energ Buildings 2007;39(2):128-35.
[3] Ryan D, Burek SAM. Experimental study of the influence of collector height on the steady state performance of a passive solar air heater. Sol Energy 2010;84(9):1676-84.
[4] Coussirat AGM, Jou E, Egusquiza E, CuervaE, Alavedra P. Performance and influence of numerical sub-models on the CFD simulation of free and forced convection in double-glazed ventilated façades. Energ Buildings 2008;40(10):1781-9.
[5] Gan G. Simulation of buoyancy-induced flow in open cavities for natural ventilation. Energ Buildings 2006;38(5):410-20.
[6] Dan CPO, Chereches C, Polidori G, Fohanno S. Flow visualization of natural convection in a vertical channel with asymmetric heating. Int Commun Heat Mass 2012;39(4):486-93.
[7] Zogou O, Stapountzis H. Flow and heat transfer inside a PV/T collector for building application. Appl Energ 2012;91(1):103-15.
[8] Bejan A. Heat Transfer. Bejan A. KAD, editor. New York: John Wiley & Sons Inc.; 1993.
[9] Kutscher CF. An investigation of heat transfer for air flow through low porosity perforated plates. Colorado: University of Colorado; 1992.
[10] Dymond C, Kutscher C. Development of a flow distribution and design model for transpired solar collectors. Sol Energy. 1997;60(5): 291-300.
[11] Augustus LM, Kumar S. Mathematical modeling and thermal performance analysis of unglazed transpired solar collectors. Sol Energy 2007;81(1):62-75.
[12] Chan H-Y. Solar facades for heating and cooling in buildings. Nottingham: University of Nottingham; 2011.
[13] Gunnewiek LH, Brundrett E, Hollands KGT. Flow distribution in unglazed transpired plate solar air heaters of large area. Sol Energy 1996;58(4-6):227-37.
[14] Kutscher CF. Heat exchange effectiveness and pressure drop for air flow through perforated plates with and without crosswinds. J Heat Transfer 1994;116:391–9.
[15] Kutscher CF, Christensen CB, Barker GM. Unglazed transpired solar collectors: heat loss theory. ASME J Sol Eng 1993;115(3):182–8.
[16] Hatami N, Bahadorinejad M. Experimental determination of natural convection heat transfer coefficient in a vertical flat-plate solar air heater Sol Energy 2008;82(10):903-10.
[17] Gao W, Lin W, Liu T, Xia C. Analytical and experimental studies on the thermal performance of cross-corrugated and flat-plate solar air heaters Appl Energ 2007;84(4):425-41.
[18] Forson FK, Nazha MAA, Rajakaruna H. Experimental and simulation studies on a single pass, double duct solar air heater. Energ Convers Manage 2003;44(8):1209-27.
[19] Ozgen F, Esen M, Esen H. Experimental investigation of thermal performance of a double-flow solar air heater having aluminium cans. Renew Energ 2009;34(11):2391-8.
[20] Prasad SB, Saini JS, Singh KM. Investigation of heat transfer and friction characteristics of packed bed solar air heater using wire mesh as packing material. Sol Energy 2009;83(5):773-83.